Berry phase and quantum entanglement in Majorana's stellar representation

H. D. Liu[1] and L. B. Fu[2,3,*]

[1]*Center for Quantum Sciences and School of Physics, Northeast Normal University, Changchun 130024, China*
[2]*National Laboratory of Science and Technology on Computational Physics, Institute of Applied Physics and Computational Mathematics, Beijing 100088, China*
[3]*HEDPS, Center for Applied Physics and Technology, Peking University, Beijing 100084, China*

(Received 9 May 2016; revised manuscript received 29 July 2016; published 31 August 2016)

By presenting the evolution of a quantum state with the trajectories of the Majorana stars on the Bloch sphere, the Majorana's stellar provides an intuitive geometric picture to study a quantum system with high-dimensional Hilbert space. We study the Berry phase and quantum entanglement by distributions and motions of these stars on the Bloch sphere. It is shown that both of these unique characters of quantum state can be perfectly represented by the Majorana stars. The former is expressed by the solid angles of Majorana star loops and the distance between stars. For the latter, the distances between stars are also found to be a tool for measuring and classifying the multiparticle entanglement of a symmetric multiqubit pure state. To demonstrate our theory, we study a typical spin model which is equivalent to an interacting boson model or an interacting multiqubit system. The self-trapping phenomenon within is also discussed via the Majorana stars.

DOI: 10.1103/PhysRevA.94.022123

I. INTRODUCTION

It is well known that the evolution of an arbitrary two-level state can be perfectly represented by the trajectory of a point on the Bloch sphere. This geometric interpretation seems hard to use for a quantum state in a high-dimensional Hilbert space. Although we can map the quantum pure state to a higher-dimensional geometric structure, this is no longer an intuitive way to comprehend it. Luckily, the Majorana's stellar representation (MSR) builds us a bridge between the high-dimensional projective Hilbert space and the two-dimensional Bloch sphere [1]. Majorana's insight was that we can describe a spin-J state (which is equivalent to an n-body two-mode boson state [2] or a symmetric n-qubit state with $n = 2J$) by $2J$ points on the two-dimensional Bloch sphere, rather than one point on a high-dimensional geometric structure. These $2J$ points are called Majorana stars of the state. Consequently, this representation rapidly meets the increasing interest in the high-dimensional or many-body system, such as spinor boson gases [3–8], multiqubit system [9], and Lipkin-Meshkov-Glick (LMG) model [10,11].

Furthermore, the MSR yields many useful insights for high-dimensional quantum states. As one unique character of a quantum state, the Berry phase [12] reveals the gauge structure associated with cyclic evolution in Hilbert space [13] and has become a central unifying concept for quantum state [14,15]. For an arbitrary two-level state, the Berry phase is simply proportional to the solid angle subtended by the close trajectory of a point on the Bloch sphere, whereas every star in the MSR will trace out its own trajectory on the Bloch sphere for a cyclic evolution of a large spin state. For example, the spin-orbit coupling in high-spin condensates can drive the Majorana stars moving periodically on the Bloch sphere, and forming the so-called "Majorana spin helix" [5]. Hence, it is natural to ask the following: can we have an explicit relation between the Berry phase and the Majorana stars' helixes or loops? It has become an interesting topic in recent years [16–20]. Hence, one of the insights the MSR brought for a quantum state is how to visualize the Berry phase of a large spin state by the trajectories of stars on the Bloch sphere such as the solid angle for the spin-$1/2$ state.

Except for the Berry phase, entanglement is another important unique character of a quantum state. Especially for the multiqubit states, the classification and measure are quite complex [21–25]. Since a spin-J state is equivalent to a symmetric $2J$-qubit state, the MSR naturally provides an intuitive way to study the multiqubit entanglement. The distribution of the Majorana stars not only reveals the relationship between the symmetry of the state and the multipartite entanglement measures, such as geometric measure [26–29] and Barycentric measure [30], but also can be used to study entanglement classes [31,32], entanglement invariants [33], and so on. Therefore, how to connect the quantum entanglement of the qubits to the distribution of the Majorana stars on the Bloch sphere is another interesting task.

In a recent paper [19], we proposed a formula for the Berry phase in MSR and established an intuitive relation between the Berry phase and the trajectories of the Majorana stars with the solid angles of the star loops and the distances between the stars on the Bloch sphere. As an extension of that work, we will detail the main result of the previous work (such as the MSR, and the Berry phase represented by the trajectories of stars) in this paper and extend the research to several new issues, such as the connection between the quantum entanglement and the distances between stars as well as the self-trapping in the interacting two-boson system.

The paper is organized as follows. In Sec. II, we introduce the MSR and its two equivalent interpretations via a two-mode boson state and the symmetric pure qubit state. In Sec. III, the formula of the Berry phase in MSR and its connection to the distributions and motions of the Majorana stars are studied in detail. Furthermore, the uniqueness of the star correlation in the Berry phases distinguished from the identical particles (boson and fermion) is discussed with some specific cases. By investigating the situation of 2, 3, and n qubits, we establish a

*lbfu@iapcm.ac.cn

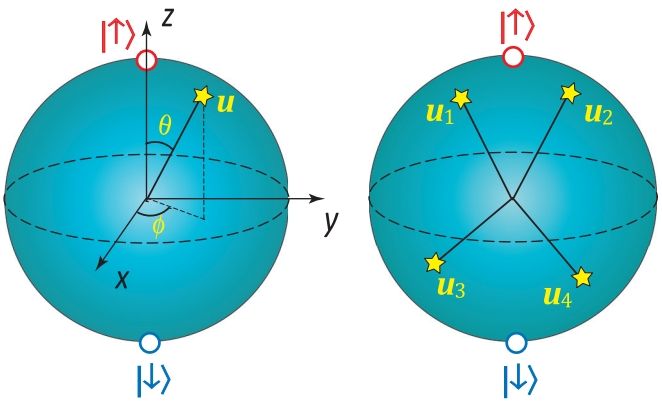

FIG. 1. Schematic illustration of stars for spin-J states on a Bloch sphere: (a) spin-1/2 and (b) spin-2. $|\uparrow\rangle$ ($|\downarrow\rangle$) denotes the spin-up (-down) state of the qubit.

relation between the distances of the stars on the Bloch sphere and the quantum entanglement of the symmetric multiqubit pure state in Sec. IV. In Sec. IV, a typical spin model which is equal to an interacting boson model or an interacting n-qubit system is studied in detail to illustrate our theory. A brief discussion and summary are given in Sec. V.

II. MAJORANA'S STELLAR REPRESENTATION

For the well-known case of a spin-1/2 system, a generic pure state

$$|\psi\rangle^{1/2} = \alpha|\uparrow\rangle + \beta|\downarrow\rangle, \tag{1}$$

represented by the basis spin-up state $|\uparrow\rangle$ and spin-down state $|\downarrow\rangle$ can be essentially defined by a complex number,

$$\lambda = \alpha/\beta = \tan\frac{\theta}{2}e^{i\phi}, \tag{2}$$

with $\theta \in [0,\pi]$ and $\phi \in [0,2\pi]$. Therefore, this state can be described by a point on the Bloch sphere with spherical coordinates (θ,ϕ) [34] [as shown in Fig. 1(a)]. More remarkably, Majorana has shown that there is also an elegant way to represent a spin-J state on the Bloch sphere by $2J$ points [1]. For a generic spin-J state,

$$|\psi\rangle^{J} = \sum_{-J}^{J} C_m|Jm\rangle, \tag{3}$$

one can establish the equation

$$\sum_{k=0}^{2J}\frac{(-1)^k C_{J-k}}{\sqrt{(2J-k)!\,k!}}x^{2J-k} = 0 \tag{4}$$

of probability amplitudes C_m with $2J$ roots $x_1,x_2,\ldots,x_{2j}$. Similar to Eq. (2), each of the roots x_k can be written as

$$x_k \equiv \tan\frac{\theta_k}{2}e^{i\phi_k}, \tag{5}$$

which correspond to $2J$ points $\boldsymbol{u}_k = (\theta_k,\phi_k)$ on the Bloch sphere [as shown in Fig. 1(b)]. Therefore, the spin-J state (3) and its evolution can be depicted by these points, which are called Majorana stars. At first appearance, this parameterizing method of the MSR seems like it can be used for any state with the Hilbert space of an arbitrary dimension [19]. Actually, the MSR is essentially an embodiment of the SU(2) symmetry and can be strictly interpreted via both a two-mode boson state and the symmetric multiqubit pure state of carrying the same SU(2) symmetries as a large spin state.

A. Two-mode boson state interpretation of MSR

For a spin-J system, it is known that the angular momentum operators can be described by the creation and annihilation bosonic operators [2]. Under Schwinger boson representation, the basis of the spin-J system $|Jm\rangle$ is equivalent to a two-mode boson state $|n_1,n_2\rangle$ with boson numbers $n_1 = J+m$ in mode 1 and $n_2 = J-m$ in mode 2. Therefore, the spin-J state (3) is equal to a generic state of an n-dimensional two-mode boson system,

$$|\Psi\rangle^{(n)} = \sum_{-n/2}^{n/2}\frac{C_m\hat{a}^{\dagger(\frac{n}{2}+m)}\hat{b}^{\dagger(\frac{n}{2}-m)}}{\sqrt{(\frac{n}{2}+m)!(\frac{n}{2}-m)!}}|\varnothing\rangle_B, \tag{6}$$

with $n = 2J$ and the vacuum state $|\varnothing\rangle_B$. Note that the sum in $|\Psi\rangle^{(n)}$ is a homogenous n-degree polynomial of bosonic operators $\hat{a}^\dagger$ and $\hat{b}^\dagger$, and it can be factorized as

$$\begin{aligned}|\Psi\rangle^{(n)} &= \frac{C_1}{\sqrt{n!}}(\hat{a}^\dagger+\lambda_1\hat{b}^\dagger)\cdots(\hat{a}^\dagger+\lambda_n\hat{b}^\dagger)|\varnothing\rangle_B \\ &= \frac{1}{N_n(\boldsymbol{U})}\prod_{k=1}^{n}\hat{a}^\dagger_{\boldsymbol{u}_k}|\varnothing\rangle_B,\end{aligned} \tag{7}$$

where $\lambda_k \equiv \tan\frac{\theta_k}{2}e^{i\phi_k}$ are the coefficients determined by the probability amplitudes C_m, and

$$N_n(\boldsymbol{U}) = \left[\frac{(n+1)!}{2^n}\sum_{k=0}^{[n/2]}\frac{D_k^n}{(2k+1)!!}\right]^{\frac{1}{2}} \tag{8}$$

is the normalization coefficient with $\boldsymbol{U} \equiv \{\boldsymbol{u}_1,\ldots,\boldsymbol{u}_{2J}\}$ and $[n/2] \equiv n/2$ ($[n/2] \equiv (n-1)/2$) for n even (n odd) [19]. The expression of symmetric function D_k^n [35] is

$$D_k^n \equiv \sum_{i_1=1}^{n}\sum_{j_1>i_1}^{n}\cdots\sum_{i_k>i_{k-1}}^{n*}\sum_{j_k>i_k}^{n*}(\boldsymbol{u}_{i_1}\cdot\boldsymbol{u}_{j_1})\cdots(\boldsymbol{u}_{i_k}\cdot\boldsymbol{u}_{j_k}), \tag{9}$$

where the $*$ indicates a restriction on the summations so that all nonrepeated indices in each term take different values. The creation operators

$$\hat{a}^\dagger_{\boldsymbol{u}_k} \equiv \cos\frac{\theta_k}{2}\hat{a}^\dagger + \sin\frac{\theta_k}{2}e^{i\phi_k}\hat{b}^\dagger \tag{10}$$

and the annihilation operators $\hat{a}_{\boldsymbol{u}_k}$ satisfy

$$\left[\hat{a}^\dagger_{\boldsymbol{u}_i},\hat{a}^\dagger_{\boldsymbol{u}_j}\right] = \left[\hat{a}_{\boldsymbol{u}_i},\hat{a}_{\boldsymbol{u}_j}\right] = 0, \quad \left[\hat{a}^\dagger_{\boldsymbol{u}_i},\hat{a}_{\boldsymbol{u}_j}\right] = \langle\boldsymbol{u}_i|\boldsymbol{u}_j\rangle, \tag{11}$$

with

$$|\boldsymbol{u}_k\rangle = \left(\cos\frac{\theta_k}{2}\hat{a}^\dagger + \sin\frac{\theta_k}{2}e^{i\phi_k}\hat{b}^\dagger\right)|\varnothing\rangle_B. \tag{12}$$

Consequently, the above factorization will give out n pairs of parameters θ_k,ϕ_k ($k = 1,\ldots,n$) which correspond to n points $\boldsymbol{u}_k = (\theta_k,\phi_k)$ on the Bloch sphere. Compare Eq. (7) with (6), we can find that the coefficients λ_k brought by the factorization

process can be derived as the roots of equation

$$\sum_{k=0}^{n} \frac{(-1)^k C_{n/2-k}}{\sqrt{(n-k)!\,k!}} \lambda^{n-k} = 0. \tag{13}$$

This equation is just the star equation (4) derived by Majorana [1].

B. Symmetric multiqubit pure state interpretation of MSR

Moreover, it is well known that the basis $\{|m\rangle\}$ of spin J can also be decomposed to the form of $2J$ qubits,

$$|J,m\rangle = \binom{2J}{J+m}^{-1} \sum_{i_1<i_2\cdots<i_{J+m}}^{2J} \sigma_{+i_1}\cdots\sigma_{+i_{J+m}}|\varnothing\rangle_Q, \tag{14}$$

where

$$\binom{2J}{J+m} = \frac{(2J)!}{(J+m)!(J-m)!} \tag{15}$$

is the binomial coefficient indexed by $2J$ and $J+m$. σ_{+i_k} is the Pauli raising operator for the i_kth qubit, and $|\varnothing\rangle_Q \equiv |\downarrow\downarrow\cdots\downarrow\rangle$. Under this decomposition, the spin basis changes into a symmetric qubit state basis. For example, the states of the spin-1 basis are equivalent to

$$|11\rangle = |\uparrow\uparrow\rangle, \quad |10\rangle = \frac{1}{\sqrt{2}}(|\uparrow\downarrow\rangle + |\downarrow\uparrow\rangle), \quad |1-1\rangle = |\uparrow\downarrow\rangle. \tag{16}$$

Thus, a spin-$n/2$ state can be factorized as a symmetric n-qubit pure state,

$$\begin{aligned}|\Psi\rangle^{(n)} &= \sum_{-n/2}^{n/2} C_m \binom{n}{n/2+m}^{-1/2} \sum_{i_1<\cdots<i_{n/2+m}} \sigma_{+i_1}\cdots\sigma_{+i_{n/2+m}}|\varnothing\rangle_Q \\ &= C_1 \sum_P (\sigma_{+P(1)}+y_1)\cdots(\sigma_{+P(n)}+y_n)|\varnothing\rangle_Q \\ &= \frac{1}{\sqrt{n!}N_n(\boldsymbol{U})} \sum_P |\boldsymbol{u}_{P(1)}\rangle|\boldsymbol{u}_{P(2)}\rangle\cdots|\boldsymbol{u}_{P(n)}\rangle,\end{aligned} \tag{17}$$

where

$$|\boldsymbol{u}_k\rangle = \cos\frac{\theta_k}{2}|\uparrow\rangle + \sin\frac{\theta_k}{2}e^{i\phi_k}|\downarrow\rangle \tag{18}$$

is the qubit state of star $\boldsymbol{u}_k = (\theta_k,\phi_k)$. The normalization coefficient $N_n(\boldsymbol{U})$ in Eq. (7) changes into $\sqrt{n!}N_n(\boldsymbol{U})$. If one denotes $\hat{a}^\dagger|\varnothing\rangle_B = |\uparrow\rangle$ and $\hat{b}^\dagger|\varnothing\rangle_B = |\downarrow\rangle$, these spin-1/2 states are just the states in Eq. (12). The sum $\sum_P$ being over all permutations P takes $1,2,\ldots,n$ to $P(1),P(2),\ldots,P(n)$. By comparing the coefficients of the last two lines in Eq. (17), we can find that the coefficients y_k satisfy

$$\sum_P y_{P(1)}y_{P(2)}\cdots y_{P(k)} = \binom{n}{k}^{1/2} \frac{C_{k-n/2}}{\sqrt{(2J)!}C_{n/2}}, \tag{19}$$

which is exactly a direct application of Vieta's formulas [31]. Thereby, the coefficients λ_k can be derived as $2J$ roots of equation

$$\sum_{k=0}^{n} \frac{(-1)^k C_{n/2-k}}{\sqrt{(n-k)!\,k!}} y^{n-k} = 0, \tag{20}$$

which is identical to Eqs. (4) and (13).

These two interpretations introduced above are mathematically equivalent since they are both restrict to the SU(2) symmetry. Therefore, the MSR provides us with an intuitive tool to study some basic quantum effects (such as dynamics, multiqubit entanglement, and the Berry phase) in the systems with high-dimensional Hilbert space which possess the SU(2) symmetry, such as a high-spin system, spin boson gases, and symmetric multiqubit system. It is worth noting that unlike the multiqubit entanglement, the dynamics and the Berry phase of a quantum state are only related to the probability amplitude C_m. Therefore, if we treat the MSR as a parameterizing process, the MSR can be used for any state in the Hilbert space of an arbitrary dimension [19]. For an n-dimensional generic state

$$|\psi\rangle^n = \sum_{m=1}^{n} C_m|m\rangle, \tag{21}$$

we can still use the roots $z_i \equiv \tan\frac{\theta_i'}{2}e^{i\phi_i'}$ of the equation

$$\sum_{l=0}^{n-1} \frac{(-1)^l C_{n-l} z^{n-1-l}}{\sqrt{(n-1-l)!l!}} = 0 \tag{22}$$

to define $n-1$ Majorana stars $\boldsymbol{u}_i = (\theta_i',\phi_i')$. These stars can also be used to study the dynamic and the Berry phase of $|\psi\rangle^n$ [36].

III. BERRY PHASE IN MSR

A. Berry phase represented by the trajectories of stars

In particular, the Berry phase is one unique character of a quantum state which can be studied by the MSR since each star $\boldsymbol{u}_k$ will trace out an independent trajectory on the sphere in an adiabatic cyclic evolution of the state $|\Psi\rangle^{(n)}$ [16]. These trajectories are cyclic or end up permuted and will form one or more closed loops. This process will naturally accumulate a Berry phase for $|\Psi\rangle^{(n)}$ [12],

$$\gamma^{(n)} = \oint -\mathrm{Im}^{(n)}\langle\Psi|d_{\boldsymbol{u}}|\Psi\rangle^{(n)}, \tag{23}$$

where the integral only depends on the geometric path in the parameter space. For the simplest case of the spin-1/2 state,

$$|\Psi\rangle^{(1)} = \cos\frac{\theta}{2}|\uparrow\rangle + \sin\frac{\theta}{2}e^{i\phi}|\downarrow\rangle, \tag{24}$$

the Berry phase takes the form [12]

$$\gamma^{(1)} = -\frac{1}{2}\oint(1-\cos\theta)d\phi = -\frac{1}{2}\Omega_{\boldsymbol{u}}, \tag{25}$$

where $\Omega_{\boldsymbol{u}}$ is the solid angle subtended by the close trajectory of star $\boldsymbol{u} = (\theta,\phi)$. The Berry phase is just proportional to the solid angle $\Omega_{\boldsymbol{u}}$. Therefore, it is interesting to ask if the Berry phase can be represented by the parameterized loops of stars when $n > 1$. In Ref. [19], it was found that the Berry phase not only includes the respective trajectories of each star, but also related to the correlations between the stars. It can be written

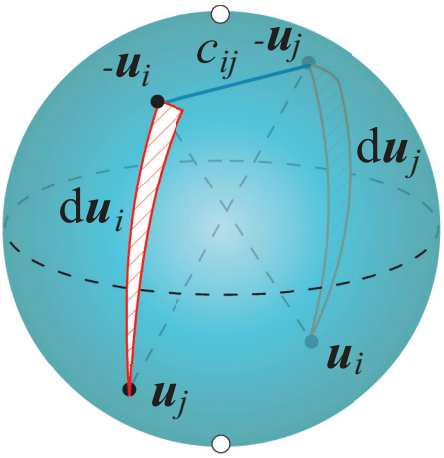

FIG. 2. Schematic illustration of solid angle $\Omega(d\boldsymbol{u}_{ij})$ (areas subtended by the red solid lines) and chordal distance c_{ij} (blue solid line).

as a sum of these two different contributions [19],

$$\gamma^{(n)} = \gamma_0^{(n)} + \gamma_C^{(n)}. \tag{26}$$

The first part is just like the situation of spin-1/2, where

$$\gamma_0^{(n)} = -\frac{1}{2}\sum_{i=1}^{n}\Omega_{\boldsymbol{u}_i} \tag{27}$$

is the sum of the solid angles

$$\Omega_{\boldsymbol{u}_i} = \oint(1-\cos\theta_i)d\phi_i \tag{28}$$

subtended by the closed evolution paths of the Majorana stars on the Bloch sphere [as Fig. 3(a) shows]. Here, we consider the situation that all stars form their own close loops. For the situation in which the individual star ends up permuted, we only need to replace the loop integral symbols in Eq. (27) by ordinary integrals since the individual star does not complete an entire loop.

The other interesting part known as the correlation phase,

$$\gamma_C^{(n)} = \frac{1}{2}\oint\sum_{i=1}^{n}\sum_{j(>i)}^{n}\beta_{ij}\Omega(d\boldsymbol{u}_{ij}), \tag{29}$$

is determined by the correlations between the stars. Specifically, $\gamma_C^{(n)}$ consists of two quantities β_{ij} and $\Omega(d\boldsymbol{u}_{ij})$. The former is called correlation factor [19]

$$\beta_{ij}(\boldsymbol{D}) \equiv -\frac{d_{ij}}{N_n^2(\boldsymbol{D})}\frac{\partial N_n^2(\boldsymbol{D})}{\partial d_{ij}}, \tag{30}$$

where $\boldsymbol{D} \equiv \{d_{ij}\}$ $(i<j)$ is a collection of

$$d_{ij} \equiv 1 - \boldsymbol{u}_i\cdot\boldsymbol{u}_j = c_{ij}^2/2, \tag{31}$$

which is related to the chordal distance c_{ij} between two stars $\boldsymbol{u}_i = (\theta_i,\phi_i)$ and $\boldsymbol{u}_j = (\theta_j,\phi_j)$ (see the blue solid line in Fig. 2) and can be defined as the "distance" between the two stars. It is easy to find that the square of the normalization coefficient $N_n(\boldsymbol{U})$ in Eq. (8) only contains the products of the first degrees of d_{ij}. For example,

$$\begin{aligned}
N_2^2(\boldsymbol{D}) &= \frac{1}{2}(3+\boldsymbol{u}_1\cdot\boldsymbol{u}_2) = \frac{1}{2}(4-d_{12}),\\
N_3^2(\boldsymbol{D}) &= 3+\boldsymbol{u}_1\cdot\boldsymbol{u}_2+\boldsymbol{u}_2\cdot\boldsymbol{u}_3+\boldsymbol{u}_3\cdot\boldsymbol{u}_1\\
&= 6-d_{12}-d_{23}-d_{13},\\
N_4^2(\boldsymbol{D}) &= \frac{15}{2}+\frac{5}{2}\sum_{i<j}^{4}\boldsymbol{u}_i\cdot\boldsymbol{u}_j+\frac{1}{2}\sum_{i<j,k<l}^{4}(\boldsymbol{u}_i\cdot\boldsymbol{u}_j)(\boldsymbol{u}_k\cdot\boldsymbol{u}_l)\\
&= 5+\frac{5}{2}\sum_{i<j}^{4}d_{ij}+\frac{1}{2}\sum_{i<j,k<l}^{4}d_{ij}d_{kl}.
\end{aligned} \tag{32}$$

It indicates that the normalization coefficient can be written as

$$N_n^2(\boldsymbol{U}) = -d_{ij}\frac{\partial N_n^2(\boldsymbol{U})}{\partial d_{ij}} + \text{terms without } d_{ij}. \tag{33}$$

Therefore, the correlation factor $\beta_{ij}(\boldsymbol{D})$ is just the weight of the d_{ij}-dependent terms to $N_n^2(\boldsymbol{D})$, i.e., the contribution of d_{ij} to $N_n^2(\boldsymbol{D})$.

The other quantity

$$\Omega(d\boldsymbol{u}_{ij}) \equiv \boldsymbol{u}_i\times\boldsymbol{u}_j\cdot d(\boldsymbol{u}_j-\boldsymbol{u}_i)/d_{ij} \tag{34}$$

in $\gamma_C^{(n)}$ can be defined as the sum of solid angles of the infinite thin triangles $(\boldsymbol{u}_i,-\boldsymbol{u}_j,-\boldsymbol{u}_j-d\boldsymbol{u}_j)$ and $(\boldsymbol{u}_j,-\boldsymbol{u}_i,-\boldsymbol{u}_i-d\boldsymbol{u}_i)$ for stars $\boldsymbol{u}_i = (\theta_i,\phi_i)$ and $\boldsymbol{u}_j = (\theta_j,\phi_j)$ [see the areas subtended by the red solid lines in Fig. (2)]. This solid angle seems hardly related to the motions of stars. To start with, we consider a simple situation with stars $\boldsymbol{u}_1 = (0,0)$, $\boldsymbol{u}_2 = (\theta,\phi)$, where the solid angle becomes

$$\Omega(d\boldsymbol{u}_{ij}) = \frac{\boldsymbol{u}_1\times\boldsymbol{u}_2\cdot d\boldsymbol{u}_2}{1-\boldsymbol{u}_1\cdot\boldsymbol{u}_2} = (1+\cos\theta)d\phi, \tag{35}$$

which is the double of the solid angles subtended by the closed trajectory of $\boldsymbol{u}_2$. Considering this situation, we can divide the motions of the two stars $\boldsymbol{u}_i = (\theta_i,\phi_i)$ and $\boldsymbol{u}_j = (\theta_j,\phi_j)$ into their absolute motions and the relative motions between them. Specifically, we can use a rotation

$$T_i = \begin{pmatrix}\cos\theta_i & 0 & -\sin\theta_i\\ 0 & 1 & 0\\ \sin\theta_i & 0 & \cos\theta_i\end{pmatrix}\begin{pmatrix}\cos\phi_i & \sin\phi_i & 0\\ -\sin\phi_i & \cos\phi_i & 0\\ 0 & 0 & 1\end{pmatrix} \tag{36}$$

to establish a moving frame in which the star $\boldsymbol{u}_i = (\theta_i,\phi_i)$ is fixed and located at z axis $\boldsymbol{Z} = (0,0)$, and $\boldsymbol{u}_j = (\theta_j,\phi_j)$ is rotated to $\boldsymbol{u}'_{j(i)} = (\theta'_{j(i)},\phi'_{j(i)})$ accordingly with [see Fig. 3(b)]

$$\begin{aligned}
\theta'_{j(i)} &= \arccos[\cos\theta_i\cos\theta_j+\sin\theta_i\sin\theta_j\cos(\phi_i-\phi_j)],\\
\phi'_{j(i)} &= \arctan\left[\frac{-\sin\theta_j\sin(\phi_i-\phi_j)}{-\cos\theta_j\sin\theta_i+\sin\theta_j\cos\theta_i\cos(\phi_i-\phi_j)}\right],
\end{aligned} \tag{37}$$

or, equivalently, fix $\boldsymbol{u}_j = (\theta_j,\phi_j)$ onto $\boldsymbol{Z} = (0,0)$, and $\boldsymbol{u}_i = (\theta_i,\phi_i)$ becomes $\boldsymbol{u}'_{i(j)} = (\theta'_{i(j)},\phi'_{i(j)})$ [see Fig. 3(c)] with

$$\begin{aligned}
\theta'_{i(j)} &= \arccos[\cos\theta_i\cos\theta_j+\sin\theta_i\sin\theta_j\cos(\phi_i-\phi_j)],\\
\phi'_{i(j)} &= \arctan\left[\frac{-\sin\theta_i\sin(\phi_j-\phi_i)}{-\cos\theta_i\sin\theta_j+\sin\theta_i\cos\theta_j\cos(\phi_j-\phi_i)}\right].
\end{aligned} \tag{38}$$

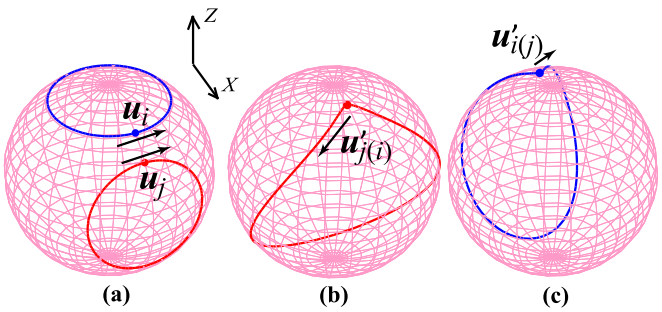

FIG. 3. A schematic illustration of (a) the absolute motions of $\boldsymbol{u}_i = (\theta_i,\phi_i)$ and $\boldsymbol{u}_j = (\theta_j,\phi_j)$ and the relative motions (b) $\boldsymbol{u}_{j(i)}$, and (c) $\boldsymbol{u}_{i(j)}$ between the two stars (see also Fig. 1 in Ref. [19]).

In these two moving frames, we can study the relative motion of $\boldsymbol{u}_i$ ($\boldsymbol{u}_j$) to $\boldsymbol{u}_j$ ($\boldsymbol{u}_i$), respectively [as Figs. 3(b) and 3(c) show].

Considering these relative motions, the solid angle $\Omega(d\boldsymbol{u}_{ij})$ in Eq. (34) becomes [19]

$$\Omega(d\boldsymbol{u}_{ij}) = (d\phi'_{i(j)} + d\phi'_{j(i)}) + (\cos\theta_i d\phi_i + \cos\theta_j d\phi_j), \tag{39}$$

where $\theta' = \theta'_{j(i)} = \theta'_{i(j)}$ is the angle between $\boldsymbol{u}_i$ and $\boldsymbol{u}_j$. Note that the solid angle subtended by the closed trajectory of a star $\boldsymbol{u} = (\theta,\phi)$ is

$$\Omega(\boldsymbol{u}) = \oint (1-\cos\theta)d\phi. \tag{40}$$

Therefore, the geometric meaning of Eq. (39) can be found as the solid angles subtended by the close trajectories of the two stars $\boldsymbol{u}_i$, $\boldsymbol{u}_j$, and the solid angle related to the relative motions between these two stars [19]. Consequently, the correlation phase $\gamma_C^{(n)}$ can be understood as the collection of the weighted relative evolutions between the stars,

$$\gamma_{Rij}^{(n)} \equiv \frac{1}{2}\oint \beta_{ij}(\boldsymbol{D})\frac{\Omega(d\boldsymbol{u}'_{i(j)}) + \Omega(d\boldsymbol{u}'_{j(i)})}{1-\boldsymbol{u}_i\cdot\boldsymbol{u}_j}, \tag{41}$$

with $\Omega(d\boldsymbol{u}'_{i(j)}) = (1-\cos\theta')d\phi'_{i(j)}$ and the collection of the weighted absolute evolutions of the pairs of stars,

$$\gamma_{Aij}^{(n)} \equiv \frac{1}{2}\oint \beta_{ij}(\boldsymbol{D})(\cos\theta_i d\phi_i + \cos\theta_j d\phi_j). \tag{42}$$

Namely,

$$\gamma_C^{(n)} = \sum_{i=1}^{n}\sum_{j(>i)}^{n}\left(\gamma_{Rij}^{(n)} + \gamma_{Aij}^{(n)}\right). \tag{43}$$

Therefore, the Berry phase in MSR consists of not only the solid angles subtended by the close trajectories of the stars, but also a correlation part consisting of the weighted solid angles subtended by the absolute motion of every star and the relative motion between each pair of stars. These correlation part stems from the nonorthogonality of two qubit states of stars. In other words, the commutation relation between the boson operators $\hat{a}^\dagger_{\boldsymbol{u}_i}$ and $\hat{a}_{\boldsymbol{u}_j}$ is $\langle\boldsymbol{u}_i|\boldsymbol{u}_j\rangle$, not δ_{ij}. This is different from the ordinary identical particles. For n bosons or fermions, the Berry phases for their symmetric (antisymmetric) many-body states are sums of the Berry phases for their single-particle states. There will be no correlation between the single-particle states.

B. Some specific cases for the Berry phase $\gamma^{(n)}$

So far, we have derived several formulas of the Berry phase in MSR. To illustrate these formulas, we discuss some specific situations for $\gamma^{(n)}$. The simplest state in MSR is that all the stars locate on one single point. The corresponding state

$$|\Psi\rangle^{(n)} = |\boldsymbol{u}_\alpha\rangle|\boldsymbol{u}_\alpha\rangle\cdots|\boldsymbol{u}_\alpha\rangle \tag{44}$$

has n coincident stars $\boldsymbol{u}_\alpha = (\theta_\alpha,\phi_\alpha)$, which is equal to the spin coherent state [17,30]

$$|\alpha\rangle_J = e^{\alpha\hat{J}_+}|j,-j\rangle, \tag{45}$$

with a complex coefficient $\alpha = \tan\frac{\theta_\alpha}{2}e^{i\phi_\alpha}$. In this situation, the stars have no correlation between each other. Therefore, the Berry phase in $\gamma^{(n)}$ will be reduced to the sum of solid angles of all stars,

$$\gamma^{(n)} = -\frac{n}{2}\Omega_{\boldsymbol{u}_i}. \tag{46}$$

Another typical situation is a spin J in a uniform magnetic field $\boldsymbol{B} = B(\sin\theta\cos\varphi, \sin\theta\cos\varphi, \cos\theta)$, which has eigenstates

$$\begin{aligned}|E_m\rangle^{(2J)} &= e^{-i\hat{J}_z}e^{-i\hat{J}_y\theta}e^{i\hat{J}_z\varphi}|Jm\rangle \\ &= \frac{e^{-i\hat{J}_z}e^{-i\hat{J}_y\theta}e^{i\hat{J}_z\varphi}\hat{a}^{\dagger(J+m)}_{\downarrow}\hat{a}^{\dagger(J-m)}_{\uparrow}}{\sqrt{(J-m)!(J+m)!}}|\varnothing\rangle_B.\end{aligned} \tag{47}$$

Using relations

$$\begin{aligned}e^{i\varphi\hat{J}_Z}\hat{a}^\dagger_{\uparrow\downarrow}e^{-i\varphi\hat{J}_Z} &= e^{\pm i\varphi/2}\hat{a}^\dagger_{\uparrow\downarrow}, \\ e^{i\theta\hat{J}_y}\hat{a}^\dagger_{\uparrow\downarrow}e^{-i\theta\hat{J}_y} &= \cos\frac{\theta}{2}\hat{a}^\dagger_{\uparrow\downarrow} \mp \sin\frac{\theta}{2}\hat{a}^\dagger_{\downarrow\uparrow},\end{aligned} \tag{48}$$

it becomes

$$\begin{aligned}|E_m\rangle^{(2J)} = \frac{e^{-i\varphi/2}}{\sqrt{(J-m)!(J+m)!}}&\left(\cos\frac{\theta}{2}\hat{a}^\dagger_\uparrow + \sin\frac{\theta}{2}e^{i\varphi}\hat{a}^\dagger_\downarrow\right)^{J+m} \\ &\times\left(\sin\frac{\theta}{2}\hat{a}^\dagger_\uparrow - \cos\frac{\theta}{2}e^{i\varphi}\hat{a}^\dagger_\downarrow\right)^{J-m}|\emptyset\rangle.\end{aligned} \tag{49}$$

Hence, $|E_m\rangle^{(2J)}$ has $J+m$ coincident stars $\boldsymbol{u} = (\theta,\varphi)$ and their $J-m$ coincident antipodal stars $\boldsymbol{u}' = (\pi-\theta,\pi+\varphi)$ with $\boldsymbol{u}\times\boldsymbol{u}' = 0$. The Berry phase thus becomes [19,37]

$$\gamma^{(2J)} = \gamma_0^{(2J)} = -\tfrac{1}{2}[(J+m)\Omega_{\boldsymbol{u}} - (J-m)\Omega_{\boldsymbol{u}'}] = -m\Omega_{\boldsymbol{u}}. \tag{50}$$

Furthermore, there is a special situation that all the distances between stars are invariant, i.e., all the stars rotate with the same angular velocity as a rigid body. Since the correlation factors β_{ij} become constants in this situation, the correlation phase $\gamma_C^{(n)}$ in Eq. (29) changes into a sum of weighted solid angles as

$$\gamma_C^{(n)} = \frac{1}{2}\sum_{i=1}^{n}\sum_{j(\neq i)}^{n}\beta_{ij}\Omega(\boldsymbol{u}_{ij}), \tag{51}$$

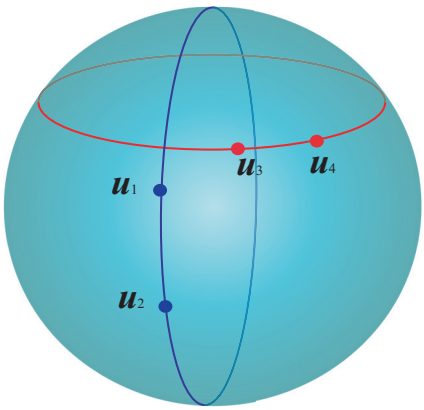

FIG. 4. Schematic illustration of stars on the same circle of longitude (blue dots on the blue circle) or latitude (red dots on the red circle).

where

$$\begin{aligned}\Omega(\boldsymbol{u}_{ij}) &\equiv \oint \Omega(d\boldsymbol{u}_{ij}) \\ &= \oint (\{d\phi'_{i(j)} + d\phi'_{j(i)}) + \oint (\cos\theta_i d\phi_i + \cos\theta_j d\phi_j) \\ &= \frac{\Omega_{\boldsymbol{u}'_{i(j)}} + \Omega_{\boldsymbol{u}'_{j(i)}}}{1 - \boldsymbol{u}_i \cdot \boldsymbol{u}_j} - [(\Omega_{\boldsymbol{u}_i} + \Omega_{\boldsymbol{u}_j}) \mathrm{mod}(2\pi)], \end{aligned} \tag{52}$$

with the solid angles $\Omega_{\boldsymbol{u}'_{i(j)}}$ ($\Omega_{\boldsymbol{u}'_{j(i)}}$) subtended by the closed evolution paths of $\boldsymbol{u}'_i$ ($\boldsymbol{u}'_j$) relative to $\boldsymbol{u}_j$ ($\boldsymbol{u}_i$), respectively. Therefore, $\Omega(\boldsymbol{u}_{ij})$ is composed of the solid angles accumulated by the relative evolution between $\boldsymbol{u}_i$ and $\boldsymbol{u}_j$ [as Figs. 3(b) and 3(c) show], and the solid angles accumulated by the evolutions of $\boldsymbol{u}_i$ and $\boldsymbol{u}_j$ themselves [as Fig. 3(a) shows].

There is also a special case which can distinguish the two parts $\gamma^{(n)}_{Rij}$ and $\gamma^{(n)}_{Aij}$ of a star pair $\boldsymbol{u}_i$ and $\boldsymbol{u}_j$. That is the two stars keeping on the same circle of longitude or latitude as shown in Fig. 4. The former means that the two stars and the z axis $\boldsymbol{Z} = (0,0)$ will always be on the same big circle of the Bloch sphere (with $\phi_i - \phi_j = 0, \pm\pi$; see the blue dots on the blue circle in Fig. 4). Therefore, the relative motions between the two stars are always on this circle, and hence accumulate no loop. Consequently, $\gamma^{(n)}_{Rij}$ will vanish. For the latter, we have $\theta_1 = \theta_2$ (see the red dots on the red circle in Fig. 4), which indicates that $\phi'_{i(j)} = (2\pi + \phi_i - \phi_j) \mod 2\pi$ and $\phi'_{j(i)} = 2\pi + \phi_j - \phi_i \mod 2\pi$, Therefore, we have

$$d\phi'_{i(j)} + d\phi'_{j(i)} = d(2\pi) = 0. \tag{53}$$

$\gamma^{(n)}_{Rij}$ will also vanish in this case.

IV. CORRELATIONS BETWEEN STARS AND QUANTUM ENTANGLEMENT

In the study of the Berry phase above, the distance d_{ij} between two stars $\boldsymbol{u}_i$ and $\boldsymbol{u}_j$ is found to play a key role. Moreover, since a spin-$n/2$ state is equal to a symmetric n-qubit pure state, these $n(n-1)/2$ correlations or distances between stars in MSR may also be connected to the entanglement of the n qubits. In particular, the symmetry of the star constellation has been proven to be an efficient tool to study the geometric measure of multiqubit entanglement [26,27,38], which also inspired an entanglement measure based on the barycenter of stars. Furthermore, the entanglement of the multiqubit is also found to be classified into different stochastic local operations and classical communication (SLOCC) classes by Majorana stars [31,32]. For example, the entanglement of three qubits has three inequivalent classes [23,24]. Thus, these correlations between stars in MSR can be taken as a different perspective for the entanglement classification and the measure of each class. Relating the constellation of stars and the measure of entanglement (such as in Ref. [26]) for each class should be an interesting task. To address this issue, we first study the cases with two and three qubits and then generalize the results to the case with n qubits.

A. Two qubits

For two qubits, a generic symmetric pure state in MSR can be factorized as

$$\begin{aligned}|\Psi\rangle^{(2)} &= C_1|\uparrow\uparrow\rangle + C_0(|\uparrow\downarrow\rangle + |\downarrow\uparrow\rangle) + C_{-1}|\downarrow\downarrow\rangle \\ &\sim \frac{1}{\sqrt{2}N_2(\boldsymbol{U})}(|\boldsymbol{u}_1\rangle|\boldsymbol{u}_2\rangle + |\boldsymbol{u}_2\rangle|\boldsymbol{u}_1\rangle), \end{aligned} \tag{54}$$

where $N_2(\boldsymbol{U}) = \sqrt{(3 + \boldsymbol{u}_1 \cdot \boldsymbol{u}_2)/2}$ is the normalization constant, C_m are the probability amplitudes ($m = 1,0,-1$), and

$$\begin{aligned}|\boldsymbol{u}_1\rangle &= \cos\frac{\theta_1}{2}|\uparrow\rangle + \sin\frac{\theta_1}{2}e^{i\phi_1}|\downarrow\rangle, \\ |\boldsymbol{u}_2\rangle &= \cos\frac{\theta_2}{2}|\uparrow\rangle + \sin\frac{\theta_2}{2}e^{i\phi_2}|\downarrow\rangle \end{aligned} \tag{55}$$

are the qubit states of star $\boldsymbol{u}_1 = (\theta_1,\phi_1)$ and $\boldsymbol{u}_2 = (\theta_2,\phi_2)$, respectively.

For two-qubit entanglement, a conventional measure is the concurrence [39]. In our situation, it reads

$$\mathcal{C} = 2\left|C_0^2 - C_1C_{-1}\right| = \frac{d_{12}}{2N_2^2(\boldsymbol{U})}, \tag{56}$$

with $d_{12} = 1 - \boldsymbol{u}_1 \cdot \boldsymbol{u}_2$. Compared with Eq. (30), the concurrence $\mathcal{C}$ is simply the correlation factor for $|\Psi\rangle^{(2)}$,

$$\beta_{12} = \mathcal{C} = d_{12}/N_2^2(\boldsymbol{U}). \tag{57}$$

Thus, the entanglement between the two qubits is determined only by the distance d_{ij} between the two stars $\boldsymbol{u}_1$ and $\boldsymbol{u}_2$. It is easy to find that if the symmetric state in Eq. (54) is separable (the two qubits are not entangled), the two stars must overlap on one point, i.e., $\boldsymbol{u}_1 = \boldsymbol{u}_2 = \boldsymbol{u}$. The state $|\Psi\rangle^{(2)}$ then takes the form

$$|\Psi\rangle^{(2)} = |\boldsymbol{u}\rangle|\boldsymbol{u}\rangle, \tag{58}$$

while the two qubits will be maximal entangled with $\mathcal{C} = 1$ when the two stars are symmetrical about the center of the Bloch sphere. The state $|\Psi\rangle^{(2)}$ becomes

$$\frac{1}{\sqrt{2}}(|\boldsymbol{u}\rangle|-\boldsymbol{u}\rangle + |-\boldsymbol{u}\rangle|\boldsymbol{u}\rangle) \tag{59}$$

where the two-qubit states are orthogonal, i.e., $\langle\boldsymbol{u}| - \boldsymbol{u}\rangle = 0$.

Without loss of generality, we take $\boldsymbol{u}_1 = (0,0)$ and $\boldsymbol{u}_2 = (\theta,0)$ as an example. The concurrence and the trajectory of $\boldsymbol{u}_2$ are show in Fig. 5. When $\theta = 0$, the two-qubit state $|\Psi\rangle^{(2)} = |\uparrow\uparrow\rangle$ is separable and two stars coincide on the north

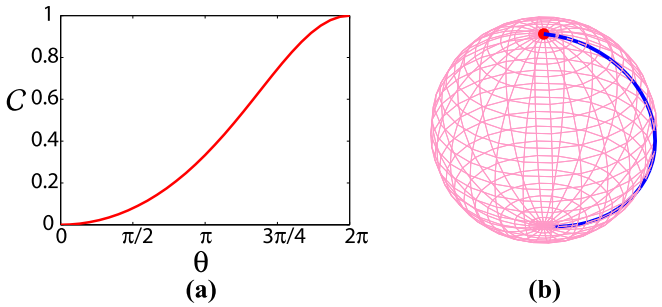

FIG. 5. (a) The concurrence $\mathcal{C}$ as a function of θ; (b) the trajectories of $\boldsymbol{u}_1$ (red dot) and $\boldsymbol{u}_2$ (blue solid line) as θ changes in (a).

pole of the Bloch sphere [as shown in Fig. 5(b)]. There is no entanglement between the two qubits. As θ changes, the concurrence $\mathcal{C}$ increases monotonically with increasing distance d_{12}. When $\theta=\pi$, $|\Psi\rangle^{(2)}$ becomes one of the Bell states (maximal entangled),

$$|\Psi\rangle^{(2)}=\frac{1}{\sqrt{2}}(|\uparrow\downarrow\rangle+|\downarrow\uparrow\rangle). \tag{60}$$

So far, the distance between two stars is related to the entanglement between two qubits. Significantly, the correlation between qubits can be perfectly represented by the correlation between stars. Moreover, if we substitute Eq. (57) into Eq. (29), the correlation phase $\gamma_C^{(2)}$ becomes

$$\gamma_C^{(2)}=\frac{1}{2}\oint\frac{\boldsymbol{u}_1\times\boldsymbol{u}_2\cdot(d\boldsymbol{u}_2-d\boldsymbol{u}_1)}{3+\boldsymbol{u}_1\cdot\boldsymbol{u}_2}=\frac{1}{2}\oint\mathcal{C}\Omega(d\boldsymbol{u}_{12}), \tag{61}$$

which means that the one from the connection of the correlation phase is a product of the concurrence $\mathcal{C}$ and the solid angle $\Omega(d\boldsymbol{u}_{12})$. This entanglement-dependent holonomic phase has become an interesting topic in recent years [40].

B. Three qubits

For three qubits, a symmetric pure state in MSR takes the form

$$\begin{aligned}|\Psi\rangle^{(3)}&=C_{\frac{3}{2}}|\uparrow\uparrow\uparrow\rangle+C_{\frac{1}{2}}(|\downarrow\uparrow\uparrow\rangle+|\uparrow\downarrow\uparrow\rangle+|\uparrow\uparrow\downarrow\rangle)\\&\quad+C_{-\frac{1}{2}}(|\uparrow\downarrow\downarrow\rangle+|\downarrow\uparrow\downarrow\rangle+|\downarrow\downarrow\uparrow\rangle)+C_{-\frac{3}{2}}|\downarrow\downarrow\downarrow\rangle\\&\sim\frac{1}{\sqrt{6}N_3(\boldsymbol{U})}(|\boldsymbol{u}_1\rangle|\boldsymbol{u}_2\rangle|\boldsymbol{u}_3\rangle+|\boldsymbol{u}_1\rangle|\boldsymbol{u}_3\rangle|\boldsymbol{u}_2\rangle\\&\quad+|\boldsymbol{u}_2\rangle|\boldsymbol{u}_1\rangle|\boldsymbol{u}_3\rangle+|\boldsymbol{u}_2\rangle|\boldsymbol{u}_3\rangle|\boldsymbol{u}_1\rangle\\&\quad+|\boldsymbol{u}_3\rangle|\boldsymbol{u}_1\rangle|\boldsymbol{u}_2\rangle+|\boldsymbol{u}_3\rangle|\boldsymbol{u}_2\rangle|\boldsymbol{u}_1\rangle),\end{aligned} \tag{62}$$

with probability amplitudes C_m ($m=3/2,1/2,-1/2,-3/2$), stars $\boldsymbol{u}_1=(\theta_1,\phi_1)$, $\boldsymbol{u}_2=(\theta_2,\phi_2)$, $\boldsymbol{u}_3=(\theta_3,\phi_3)$, and the normalization coefficient $N_3(\boldsymbol{U})=\sqrt{3+\boldsymbol{u}_1\cdot\boldsymbol{u}_2+\boldsymbol{u}_2\cdot\boldsymbol{u}_3+\boldsymbol{u}_3\cdot\boldsymbol{u}_1}$.

The entanglement of three qubits is more complex than that of two qubits [21–23]. Since three qubits can be entangled in two inequivalent ways, the three-qubit pure state can be classified into four different types [23]: (i) the class S of separable states; (ii) the class B of a bipartite entangled state, e.g., $|\downarrow\rangle(\alpha|\uparrow\uparrow\rangle+\beta|\downarrow\downarrow\rangle)$; (iii) the class W of W states [23],

$$|W\rangle_3=\frac{1}{\sqrt{3}}(|\uparrow\downarrow\downarrow\rangle+|\downarrow\uparrow\downarrow\rangle+|\uparrow\uparrow\downarrow\rangle); \tag{63}$$

and (iv) the class GHZ of GHZ states [41],

$$|\mathrm{GHZ}\rangle_3=\frac{1}{\sqrt{2}}(|\downarrow\downarrow\downarrow\rangle+|\uparrow\uparrow\uparrow\rangle). \tag{64}$$

States in these classes can be converted into each other under the SLOCC if and only if they are in the same class [23]. It can be enforced by the fact that two states are equivalent under SLOCC if an invertible local operation (ILO) relating them exists [23,26]. For symmetric pure states $|\Psi\rangle^{(3)}$, the bipartite entangled states are absent due to the permutation symmetry of the qubits. Therefore, we have three classes for the symmetric pure three-qubit states: the separable class, the W class, and the GHZ class. Furthermore, the permutation symmetry makes the search for these ILOs easier. Specifically, if two state $|\psi\rangle_3$ and $|\phi\rangle_3$ belong to the same SLOCC class, we can find a symmetric ILO which satisfies [31,32]

$$|\phi\rangle_3=A\otimes A\otimes A|\psi\rangle_3, \tag{65}$$

with the same invertible operator A on each qubit.

For three coincident stars, the separable state takes the form

$$|S\rangle_3=|\boldsymbol{u}\rangle|\boldsymbol{u}\rangle|\boldsymbol{u}\rangle. \tag{66}$$

Obviously, the state remains separable under any invertible operator A_S.

For two coincident stars, the state (62) can be written as

$$\begin{aligned}|\psi_W\rangle_3&=\frac{1}{\sqrt{6}N_3(\boldsymbol{U})}(|\boldsymbol{u}_2\rangle|\boldsymbol{u}_1\rangle|\boldsymbol{u}_1\rangle+|\boldsymbol{u}_1\rangle|\boldsymbol{u}_2\rangle|\boldsymbol{u}_1\rangle\\&\quad+|\boldsymbol{u}_1\rangle|\boldsymbol{u}_1\rangle|\boldsymbol{u}_2\rangle),\end{aligned} \tag{67}$$

with $\boldsymbol{u}_3=\boldsymbol{u}_1$ and $N_3(\boldsymbol{U})=\sqrt{4+2\boldsymbol{u}_1\cdot\boldsymbol{u}_2}$. We can always find an invertible operator A_W transforming $|\boldsymbol{u}_1\rangle$ into $|\uparrow\rangle$ and $|\boldsymbol{u}_2\rangle$ into $|\downarrow\rangle$ with

$$A_W\equiv\begin{pmatrix}\cos\frac{\theta_1}{2} & \cos\frac{\theta_2}{2}\\ \sin\frac{\theta_1}{2}e^{i\phi_1} & \sin\frac{\theta_2}{2}e^{i\phi_2}.\end{pmatrix}^{-1}. \tag{68}$$

Therefore, this type of state can be transformed into the W state (63).

For three separated stars $\boldsymbol{u}_1$, $\boldsymbol{u}_2$, and $\boldsymbol{u}_3$ of the state $|\Psi\rangle^{(3)}$, an invertible operator A_G can also be determined by [31]

$$\begin{aligned}\frac{e}{\sqrt{2}}(|\uparrow\rangle+|\downarrow\rangle)&=A_G|\boldsymbol{u}_1\rangle,\\\frac{f}{\sqrt{2}}(|\uparrow\rangle+e^{i2\pi/3}|\downarrow\rangle)&=A_G|\boldsymbol{u}_2\rangle,\\\frac{g}{\sqrt{2}}(|\uparrow\rangle+e^{i4\pi/3}|\downarrow\rangle)&=A_G|\boldsymbol{u}_3\rangle,\end{aligned} \tag{69}$$

with three complex numbers e, f, and g satisfying $efg=1$. Thus, the state $|\Psi\rangle^{(3)}$ with three separated stars can be transformed into the GHZ state $|\mathrm{GHZ}\rangle_3$ by the ILO $A_G\otimes A_G\otimes A_G$.

Moreover, an invertible operator A cannot transform two different qubit states into the same one, which means that an ILO cannot change the number of unequal stars. Thus, the dimension of the star constellation is unchanged under an

ILO [31,42]. Therefore, we can find three different classes of states with different numbers of unequal stars which can be transformed into a separable state, W state, and GHZ state, respectively. This indicates that the classes of the entanglement can be determined by the number of unequal stars. Since we have confirmed the classification of the entanglements, the next task is to find the relation between the distribution of stars and the entanglement measure for each type.

For a GHZ type of states, a valid measure of the entanglement is the three-tangle [21]. To our symmetric state (62), it takes the form

$$\tau = 4\left|\left(C_{\frac{3}{2}}C_{-\frac{3}{2}}-C_{\frac{1}{2}}C_{-\frac{1}{2}}\right)^2-\left(C_{\frac{1}{2}}^2-C_{\frac{3}{2}}C_{\frac{1}{2}}\right)\left(C_{-\frac{1}{2}}^2-C_{-\frac{3}{2}}C_{-\frac{1}{2}}\right)\right| = \frac{2d_{12}d_{23}d_{31}}{3N_3^4(\boldsymbol{U})}, \tag{70}$$

where the distance $d_{ij} = 1 - \boldsymbol{u}_i \cdot \boldsymbol{u}_j$. Like the entanglement of two qubits, the 3-tangle can also be represented by the product of the distances between the stars. For the GHZ state (64), we have $\tau = 1$. The three qubits are maximally entangled with three stars $\boldsymbol{u}_1 = (\pi/2,0)$, $\boldsymbol{u}_2 = (\pi/2,2\pi/3)$, and $\boldsymbol{u}_3 = (\pi/2,4\pi/3)$ distributing evenly on the equator of the Bloch sphere. Obviously, to ensure τ has nonzero value, the three stars should be separated from each other.

For $\tau = 0$, there are two situations: all three stars coincide on one point and two of the three stars are coincident, which corresponds to the two classes left: S class and W class. Similar to the situation of two qubits, the symmetry requires three coincident stars for the separable type of state $|S\rangle_3$. Obviously, the situation of two coincident stars is related to the W type of states. Its entanglement can be measured by the concurrence of the mixed state derived by tracing over any qubit from the density matrix of the symmetric three-qubit pure state [21], and the concurrence

$$\mathcal{C}_{12} = \frac{2(1-\boldsymbol{u}_1\cdot\boldsymbol{u}_2)}{3(4+2\boldsymbol{u}_1\cdot\boldsymbol{u}_2)} = \frac{2d_{12}}{3N_3^2(\boldsymbol{U})} \tag{71}$$

is essentially equivalent to the concurrence (56), except for its maximal value 2/3. This means that the W-type states are reduced to "two-qubit entanglement" (concurrence). Accordingly, the correlation phase $\gamma_C^{(3)}$ satisfies $\gamma_C^{(3)} = \frac{3}{2}\oint \Omega(d\boldsymbol{u}_{12})\mathcal{C}_{12}$, which is similar to Eq. (61). In brief, these three classes of entanglement S class, W class, and GHZ class can be represented by three kinds of star distributions on the Bloch sphere: three stars coincide on one point [see Fig. 6(a)], two of the three stars coincide on one point [see Fig. 6(b)], and the three stars are separated from each other [see Fig. 6(c)], respectively.

To illustrate these three types of states, we take the symmetric three-qubit states $|\psi_3\rangle$ with stars $\boldsymbol{u}_1 = (\theta,0)$, $\boldsymbol{u}_2 = (\pi-\theta,\phi/2)$, and $\boldsymbol{u}_3 = (\pi-\theta,2\pi-\phi/2)$ as an example. Its three-tangle τ are shown in Fig. 7. For $\theta = 0$ or $\psi = 0$, we have zero-valued τ; these states $|\psi_3\rangle$ thus belong to the W type, such as the W state (63) with $\theta = 0$, the Dicke state

$$|S(3,2)\rangle = \frac{1}{\sqrt{3}}(|\downarrow\uparrow\uparrow\rangle + |\uparrow\downarrow\uparrow\rangle + |\uparrow\uparrow\downarrow\rangle) \tag{72}$$

with $\theta = \pi$, and a local unitary operated W state

$$|\tilde{W}\rangle = e^{i\theta\hat{\sigma}_y/2}\otimes e^{i\theta\hat{\sigma}_y/2}\otimes e^{i\theta\hat{\sigma}_y/2}|W\rangle \tag{73}$$

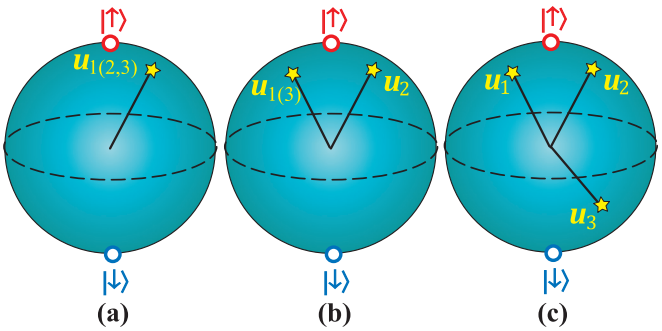

FIG. 6. Schematic illustration of stars on the Bloch sphere for the three types of entanglement for the symmetric three-qubit pure state: (a) S type, (b) W type, and (c) GHZ type.

with $\phi = 2\pi$, which has the stars $\boldsymbol{u}_1 = (\theta,0)$ and its two overlapped antipodal stars $-\boldsymbol{u}_1 = (\pi-\theta,\pi)$. When θ changes, these two noncoincident stars will always keep a maximal distance, and hence this W-type state always has the maximal entanglement $\mathcal{C} = 2/3$ as the W state [see the green line in Fig. 7(a) and the third sphere in Fig. 7(c)]. This can be explained by the fact that a local unitary transformation can be treated as a rotation of the total constellation (or, equivalently, a rotation of the Bloch sphere [27,42]) and hence cannot deform the constellation. Therefore, a local unitary operation leaves the distances between stars unchanged and cannot change the entanglement degree of the state.

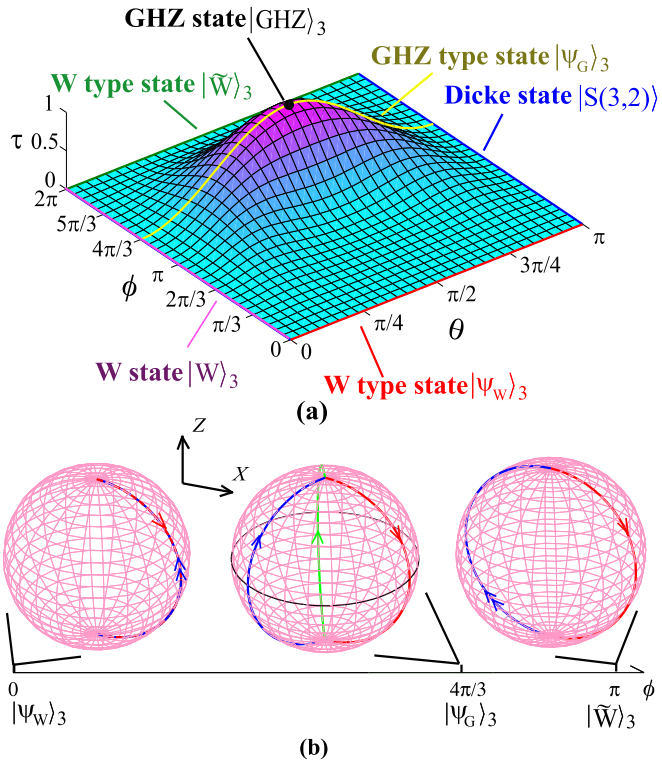

FIG. 7. (a) Three-tangle of symmetric three-qubit states $|\phi(\theta,\phi)\rangle_3$ with stars: $(\theta,\ 0)$, $(\pi-\theta,\ \phi/2)$, and $(\pi-\theta,\ 2\pi-\phi/2)$. (b) Concurrence of symmetric three-qubit W-type state $|\phi_W\rangle_3$. (c) The trajectories of stars for the W-type state $|\Psi_W\rangle_3$, GHZ-type state $|\psi_G\rangle_3$, and W-type state $|\tilde{W}\rangle$ as θ changes from 0 to π.

For $\phi = 0$, we have the W-type state $|\psi_W\rangle_3$ in Eq. (67) with star $\boldsymbol{u}_2 = (\theta,0)$ and two coincident stars $\boldsymbol{u}_1 = \boldsymbol{u}_3 = (\pi - \theta,0)$. As θ changes from 0 to π, $\boldsymbol{u}_1$ travels from the north pole to the south pole of the Bloch sphere and the other two stars travel from the south pole to the north pole. Their distances are determined by $d_{12} = 1 + \cos(2\theta)$ and the concurrence $\mathcal{C}$ becomes

$$\mathcal{C} = \frac{1 + \cos(2\theta)}{3[2 - \cos(2\theta)]}. \tag{74}$$

When $\theta = 0$ and $\theta = \pi$, the W-type states will have the maximal entanglement $\mathcal{C} = 2/3$ (see Fig. 7) and become the W state $|W\rangle_3$ (with two stars on the south pole and one star on the north pole) and the Dicke state $|S(3,2)\rangle$ (with one star on the south pole and two stars on the north pole), respectively. Moreover, when $\theta = \pi/2$, the three stars coincide on one point $\boldsymbol{u} = (\pi/2,0)$, and the state $|\psi_W\rangle_3$ becomes a separable state,

$$|S\rangle_3 = \frac{1}{2\sqrt{2}}(|\uparrow\rangle + |\downarrow\rangle)(|\uparrow\rangle + |\downarrow\rangle)(|\uparrow\rangle + |\downarrow\rangle), \tag{75}$$

which corresponds to a zero $\mathcal{C}$ (see Fig. 7).

When $\theta \neq 0$ and $\phi \neq 0$, τ has nonzero values. In this situation, $|\psi_3\rangle$ belongs to the GHZ type. Taking $\phi = 4\pi/3$ as an example, as θ changes from 0 to π, the state evolves from the W state to the Dicke state $|S(3,2)\rangle$. All of the states among these two points are GHZ-type state $|\psi_G\rangle_3$ with stars $\boldsymbol{u}_1 = (\theta,0)$, $\boldsymbol{u}_2 = (\pi - \theta,3\pi/2)$, and $\boldsymbol{u}_3 = (\pi - \theta,4\pi/2)$ [see the yellow line in Fig. 7(a) and the second sphere in Fig. 7(c)]. Especially when $\theta = \pi/2$, $|\psi_G\rangle_3$ becomes the $|\mathrm{GHZ}\rangle_3$ state (64) with three evenly distributed stars on the equator of the Bloch sphere [see the black point in Fig. 7(a) and the second sphere in Fig. 7(c)].

We find that the three different types of symmetric three-qubit pure states can be classified and measured by the distance between stars: the separable states have three coincident stars, the states of the GHZ class have three separated stars which can be measured by three-tangle, and the state of the W class, which has two coincident stars, does not have "three-qubit entanglements" (three-tangles) and their entanglements are reduced to "two-qubit entanglements" (concurrences).

C. n qubits

In the last two subsections, it has been found that the entanglements of symmetric pure states with two and three qubits are related to the distances between stars. The entanglement types can be classified by the number of unequal stars (or diversity degree of the state [31]), and measured by a normalized product of the distance between unequal stars [product of distances divide a normalization coefficient, such as three-tangle (70) and concurrence (56) and (71)]. For $n(>3)$ qubits, both the MSR and the measure of multiqubit entanglement are complex [27,30,31,33]. However, it can be proven that the entanglement types can still be classified by the number of unequal stars n_s [31], such as S type ($n_s = 1$), W type ($n_s = 2$), and GHZ type ($n_s = n$). Next, we begin with some classical types of states and then discuss the multiqubit entanglement.

The simplest case is where the state $|S\rangle$ is separable, and the symmetry of the symmetric n-qubit pure state requires that all the stars of $|S\rangle$ should be overlapped on one point $\boldsymbol{u}_S$ (see the red star in Fig. 8). Therefore, $|S\rangle$ takes the form

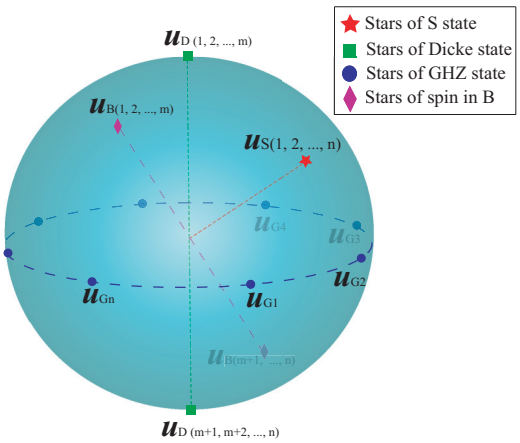

FIG. 8. Stars of several n-qubit states: separable states (red point), Dicke state (green points), GHZ state (blue points), and states of spin-J in magnetic field (purple points).

$$|S\rangle = |\boldsymbol{u}_S\rangle|\boldsymbol{u}_S\rangle\cdots|\boldsymbol{u}_S\rangle, \tag{76}$$

which is just equal to the coherent state (45) with one overlapped star, $\boldsymbol{u}_S = (\theta_S,\Phi_S)$. For the W type with two unequal stars, a typical state is the Dicke state (including the W state when $m = 1$),

$$|S(n,m)\rangle = \sum_P |\underbrace{\uparrow\uparrow\ldots\uparrow}_{m}\underbrace{\downarrow\downarrow\ldots\downarrow}_{n-m}\rangle, \tag{77}$$

where $\sum_P$ denotes taking over all permutations of spin up $\uparrow$ and spin down $\downarrow$. $|S(n,m)\rangle$ can be represented by m stars on the north pole and $n - m$ stars on the south pole (see the green squares in Fig. 8). Another kind of W-type states is the eigenstates of a spin $n/2$ in a uniform magnetic field in Eq. (47), which is equal to

$$|E_m\rangle^{(n)} = \sum_P \underbrace{|\boldsymbol{u}\rangle|\boldsymbol{u}\rangle\ldots|\boldsymbol{u}\rangle}_{n/2+m}\underbrace{|-\boldsymbol{u}\rangle|-\boldsymbol{u}\rangle\ldots|-\boldsymbol{u}\rangle}_{n/2-m}, \tag{78}$$

with $J + m$ coincident stars $\boldsymbol{u} = (\theta,\varphi)$ and their $J - m$ coincident antipodal stars $-\boldsymbol{u} = (\pi - \theta,\pi + \varphi)$ (see the purple diamonds in Fig. 8).

For a generic W-type state, $|\Psi_2\rangle^{(n)}$ with m stars $\boldsymbol{u}_1(\theta_1,\phi_1)$ and $n - m$ stars $\boldsymbol{u}_2 = (\theta_2,\phi_2)$ since the rotating operation does not change the distance between the two unequal stars. Without loss of generality, we chose $\boldsymbol{u}_1 = (0,0)$ and $\boldsymbol{u}_2 = (\theta,0)$, where $\theta = \arccos(\boldsymbol{u}_1 \cdot \boldsymbol{u}_2)$ is the angle between $\boldsymbol{u}_1$ and $\boldsymbol{u}_2$. By tracing out any $n - 2$ qubits from the density matrix ${}^{(n)}\langle\Psi_2|\Psi_2\rangle^{(n)}$, we obtain the reduced density matrix of the left two qubits. After a straightforward calculation, its concurrence reads

$$\begin{aligned} \mathcal{C}_{12}^n &= \frac{(n-2)!m(n-m)(1-\cos\theta)}{nN_n^2(\boldsymbol{U})} \\ &= \frac{(n-2)!m(n-m)d_{12}}{nN_n^2(\boldsymbol{U})}, \end{aligned} \tag{79}$$

which is in accordance with the results (56) for two qubits ($n = 2, m = 1$) and (71) for three qubits ($n = 3, m = 1$). Since the distance d_{ij} is inversely correlated to the normalization

coefficient $N_n^2(\boldsymbol{U})$, the concurrence $\mathcal{C}_{12}^n$ is a monotonic function of d_{ij}. For the Dicke states $|S(n,m)\rangle$ and the state $|E_m\rangle^{(n)}$, which have the maximal-distanced two unequal stars and $N_n^2(\boldsymbol{U}) = n!(n-m)!$, their entanglements reach the maximal value,

$$\mathcal{C}_{\max}^n = \frac{2}{n}\binom{n-2}{m-1}, \tag{80}$$

which matches the results $\mathcal{C} = 1$ for two qubits and $\mathcal{C} = 2/3$ for the W type of three qubits. Therefore, the Dicke states $|S(n,m)\rangle$ and the state $|E_m\rangle^{(n)}$ are the maximal-entangled W-type states.

For the GHZ type, all the stars are separated from each other. For example, the GHZ state

$$|\mathrm{GHZ}\rangle_n = |\uparrow\uparrow\ldots\uparrow\rangle + e^{i\phi}|\downarrow\downarrow\ldots\downarrow\rangle \tag{81}$$

has n separated stars $\boldsymbol{u}_k = (\pi/2, \phi + 2\pi/k)$ $(k = 0,1,\ldots,n-1)$ distributing evenly on the equator of the Bloch sphere and is a maximal-entangled GHZ-type state.

So far, it is known that the type of entanglement can be classified by the number of unequal stars, and can be measured by the product of distance between stars. Therefore, the normalized product of the distances between unequal stars,

$$\left(\prod_{\substack{i,j=1\\ i<j}}^{n_s} d_{ij}\right)/N_n^{2(n_s-1)}, \tag{82}$$

may be a valid measure of entanglement.

V. TWO-MODE INTERACTING BOSON SYSTEM

To illustrate our theory, we consider a typical model with Hamiltonian

$$H = \hat{\boldsymbol{J}}\cdot\boldsymbol{R} + \lambda\hat{J}_z^2, \tag{83}$$

where $\boldsymbol{R} = (\sin\theta\cos\varphi, \sin\theta\cos\varphi, \cos\theta)$, and $\hat{\boldsymbol{J}} = (\hat{J}_x, \hat{J}_y, \hat{J}_z)$ is the spin-J vector. This model exhibits rich physics and can interpret many typical systems. For example, an interacting boson system [10,43] with the Hamiltonian

$$H_{\mathrm{BS}} = \frac{R\sin\theta}{2}(e^{i\varphi}\hat{a}^\dagger\hat{b} + e^{-i\varphi}\hat{b}^\dagger\hat{a}) + \frac{R\cos\theta}{2}(\hat{a}^\dagger\hat{a} - \hat{b}^\dagger\hat{b}) + \frac{\lambda}{4}(\hat{a}^\dagger\hat{a} - \hat{b}^\dagger\hat{b})^2, \tag{84}$$

which can be derived from the bosonic-field Hamiltonian [43], has received extraordinary attention in the literature on BECs [44]. The parameters $R\cos\theta$ can be considered as the energy offset between the two modes, $R\sin\theta e^{i\varphi}$ measures the coupling between the two modes, $\lambda = g/V$ with g is the interaction strength between bosons, and V is the volume of the system. Furthermore, this mode can also be treated as an interacting n-qubit system for [45]

$$\hat{J}_\alpha = \frac{1}{2}\sum_{k=1}^{n}\hat{\sigma}_{k\alpha}, \quad \alpha = x,y,z, \tag{85}$$

where $\hat{\sigma}_{k\alpha}$ are the Pauli matrices for the kth particle.

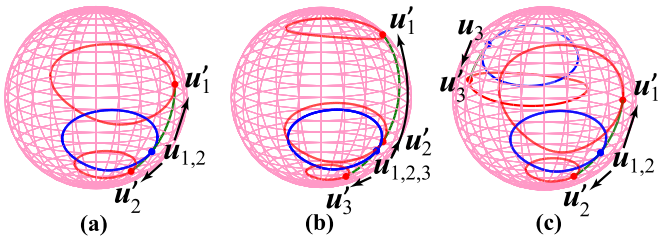

FIG. 9. The trajectories of the Majorana stars with $\lambda = 0$ (blue loops on the spheres) and $\lambda/R = 0.9$ (red loops on the spheres) for (a) ground state $|E_1\rangle^{(2)}$ of $H_{(\mathrm{BS})}$ with two bosons, (b) ground state $|E_1\rangle^{(3)}$, and (c) the first excited state $|E_2\rangle^{(3)}$ of three bosons. The evolution of θ and φ in parameter space is the same as Fig. 2 in Ref. [19].

A. Berry phase and entanglement

For $\lambda = 0$, the Hamiltonian $H_{(\mathrm{BS})}$ describe the model of a spin $n/2$ in a magnetic field $\boldsymbol{R}$ whose eigenstates are shown in Eq. (49). Therefore, there are m coincident stars $\boldsymbol{u} = (\theta,\varphi)$ and their $n-m$ coincident antipodal stars $-\boldsymbol{u} = (\pi-\theta,\pi+\varphi)$ for the mth eigenstate $|E_m\rangle^{(n)}$. Accordingly, its Berry phase $\gamma^{(n)}$ becomes

$$\gamma = (n-2m)\Omega_{\boldsymbol{u}}, \tag{86}$$

e.g., $2\Omega_{\boldsymbol{u}}$ for the ground state $|E_1\rangle^{(2)}$ with two bosons [subtended by the blue loop of $\boldsymbol{u} = \boldsymbol{u}_{1,2}$ in Fig. 9(a)], $3\Omega_{\boldsymbol{u}}$ for the ground state $|E_1\rangle^{(3)}$ of three bosons [subtended by the blue loop of $\boldsymbol{u} = \boldsymbol{u}_{1,2,3}$ in Fig. 9(b)], and $\Omega_{\boldsymbol{u}}$ for the first excited state $|E_2\rangle^{(3)}$ of three bosons [subtended by the blue loop of $\boldsymbol{u} = \boldsymbol{u}_{1,2} = -\boldsymbol{u}_3$ in Fig. 9(c)], respectively. Furthermore, the equivalent symmetric n-qubit pure state of $|E_m\rangle^{(n)}$ has already been proven to be a maximal-entangled W-type state with

$$\mathcal{C}_{\max}^n = \frac{2}{n}\binom{n-2}{m-1}. \tag{87}$$

For nonzero λ, the eigenproblem is hard to solve [10]. However, if we take λ as a perturbation ($\lambda \ll 2R$) in the simplest case of two bosons (or spin 1, or two qubits), the eigenproblem of $H_{(\mathrm{BS})}$ can be solved analytically with eigenvalues $E = -R, 0$, or R under first-order approximation.

Correspondingly, the two stars $\boldsymbol{u}_1 = (\theta_1,\phi_1)$ and $\boldsymbol{u}_2 = (\theta_2,\phi_2)$ of the eigenstate $|E_0\rangle$ for $E_0 = 0$ are determined by

$$\begin{aligned}
\theta_1 &= 2\arctan\left(\frac{R\cos\theta + \sqrt{R^2 - \lambda^2\sin^2\theta\cos^2\theta}}{(R-\lambda\cos\theta)\sin\theta}\right),\\
\phi_1 &= \pi + \varphi;\\
\theta_2 &= 2\arctan\left(\frac{-R\cos\theta + \sqrt{R^2 - \lambda^2\sin^2\theta\cos^2\theta}}{(R-\lambda\cos\theta)\sin\theta}\right),\\
\phi_2 &= \varphi,
\end{aligned} \tag{88}$$

which is just the situation in which the two stars are on the same circle of longitude, like the blue dots on the blue circle in Fig. 4. Suppose the system evolves adiabatically with parameters θ and φ; the two parts of the Berry phase $\gamma^{(n)}$ can thus be written

as

$$\gamma_0^{(2)} = -\frac{1}{2}(\Omega_{\boldsymbol{u}_1} + \Omega_{\boldsymbol{u}_2}) = \oint \left(-1 + \frac{\lambda \cos\theta \sin^2\theta}{R}\right) d\varphi,$$

$$\gamma_C^{(2)} = \gamma_{Aij}^{(2)} = \frac{1}{2}\oint \mathcal{C}(\cos\theta_1 d\phi_1 + \cos\theta_2 d\phi_{j2}), \tag{89}$$

where

$$\mathcal{C} = \frac{4R^2 - \lambda^2 \sin^2 2\theta}{4R^2 + \lambda^2 \sin^2 2\theta} \tag{90}$$

is the concurrence for the equivalent symmetric two-qubit states,

$$|\Psi\rangle^{(2)} = \frac{1}{\sqrt{3 + \boldsymbol{u}_1 \cdot \boldsymbol{u}_2}}(|\boldsymbol{u}_1\rangle|\boldsymbol{u}_2\rangle + |\boldsymbol{u}_2\rangle|\boldsymbol{u}_1\rangle), \tag{91}$$

of $|E_0\rangle$. When the coupling constant $\lambda = 0$, the two stars are antipodal with each other, which makes $|\Psi\rangle^{(2)}$ a maximal entangled state. In this case, we have $\Omega_{\boldsymbol{u}_1} = -\Omega_{\boldsymbol{u}_2}$ and $\gamma_C^{(2)} = 0$, and there is only a trivial Berry phase (0 or 2π).

For more general situations of nonzero λ, we can numerically calculate the parameter-dependent eigenstates of H. Similar to the results of the LMG model in Ref. [10], the instantaneous eigenstate of H has two groups of stars spreading over two curves on the Bloch sphere, respectively. The mth eigenstate $|E_m\rangle^{(n)}$ has $n + 1 - m$ on one curve and $m - 1$ on the other curve [10,19].

As the adiabatic parameters evolve, the time-dependent eigenstates vary accordingly. Since the existence of λ makes the stars separate from each other, their trajectories become several separated loops (see the red loops in Fig. 9) and the correlation phases arise. However, the phase $\gamma_R^{(n)}$ caused by the relative motions between stars will vanish due to the symmetry between the stars on the two curves. For example, the stars for $|E_1\rangle^{(2)}$, $|E_1\rangle^{(3)}$, and $|E_2\rangle^{(3)}$ will always locate on the same circle of longitude, as shown by the green lines in Fig. 9.

In addition, we can also see the different entanglement classes of the equivalent two- and three-qubit pure states, e.g., the S type and W type of two qubits with coincident stars and separated stars, respectively [as shown in Fig. 9(a), and the S type, W type, and GHZ type of three qubits with three coincident stars, two coincident stars, or three separated stars, respectively [as shown in Figs. 9(b) and 9(c).

B. Self-trapping in MSR

In addition to the adiabatic evolution and quantum entanglement, the dynamics of the system with Hamiltonian (83) or (84) is also an interesting issue that can be observed by the Majorana stars. Especially for $\phi = 0$ and $\theta = \pi/2$, this Hamiltonian can be used to describe the model for two-mode Bose-Einstein condensates (BECs) coupled via Josephson tunneling [44,46,47]. The Hamiltonian takes the form

$$H_2 = \frac{\lambda}{4}(n_a - n_b)^2 + \frac{R}{2}(\hat{a}^\dagger \hat{b} + \hat{b}^\dagger \hat{a}), \tag{92}$$

where $n_a = \hat{a}^\dagger \hat{a}$ and $n_b = \hat{b}^\dagger \hat{b}$ are the number operators for the two-mode condensates a and b, respectively, and the total boson number $n = n_a + n_b$ is conserved.

A well-known dynamics effect of this system is that the oscillation of the BECs between the two wells will change from delocalization into self-trapping as the nonlinearity strength increases [44,46–49]. If we choose $|n,0\rangle$ as the initial state, i.e., all the bosons are located in well a, for the linear situation with $\lambda = 0$, the BECs will oscillate between the two wells (see the green thick solid line in Fig. 10). In MSR, this corresponds to n coincident stars traveling from the north pole to the south pole and then returning to the north pole, back and forth, as shown on the first sphere in Fig. 10. When the nonlinear strength is small (for example, $n\lambda/R = 0.1$), the BECs can still be totally tunneled from one well to another well, and get back (see the black dashed line in Fig. 10). Accordingly, although the overlap of stars is broken by the nonlinearity, there are still some stars that can arrive at the south pole (see the second sphere in Fig. 10). Interestingly, when the nonlinear strength exceeds the certain threshold value $n\lambda/R = 2$, the Josephson oscillation between the two wells will be blocked (see the blue dash-dotted line in Fig. 10), and the BECs will always be collected more into well a than into well b, i.e., the expectation value of the boson number $\langle n_a \rangle$ in well a will always be larger than $\langle n_b \rangle$ in well b. The self-trapping phenomenon occurs. All of the stars cannot reach the south pole (see the third sphere in Fig. 10). As the nonlinear strength become large enough (for example, $n\lambda/R = 10$), the oscillation of the relative number between the two wells tends to be extremely small (see the red thin solid line in Fig. 10), such as the BECs are trapped in well a from the beginning. Corresponding to this interesting phenomenon, all the stars can only travel on the northern hemisphere, as shown on the fourth sphere in Fig. 10. Thus, the process of the BECs changing from delocalization into self-trapping can be intuitively represented by the range of the star motions on the Bloch sphere.

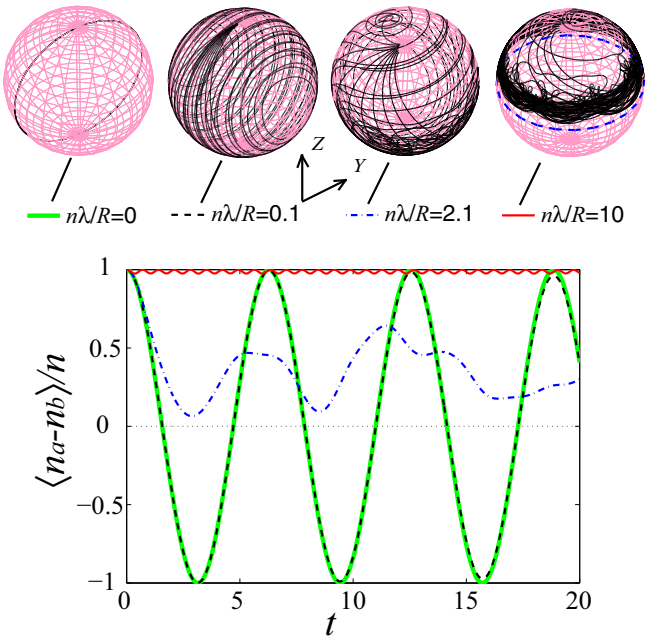

FIG. 10. The trajectories of Majorana stars and the time evolution of the relative number of expectation values with different nonlinear strengthes: $n\lambda/R = 0$ (green thick solid line), $n\lambda/R = 0.1$ (black dashed line), $n\lambda/R = 2.1$ (blue dash-dotted line), and $n\lambda/R = 10$ (red thin solid line) with the total boson number $n = 10$.

VI. DISCUSSION

The recent research on the Majorana's stellar representation has indicated that the distributions and motions of the Majorana stars on the Bloch sphere have become a new tool to study the symmetry-related questions in the high-dimensional or many-body system. Our detailed study here shows that the two important unique characteristics of a quantum state, i.e., the Berry phase and quantum entanglement, can be represented intuitively by the loops of stars and the distances between them. The Berry phase not only consists of the solid angles subtended by every Majorana star's trajectories on the Bloch sphere, but is also associated with the correlation between the stars. These correlations between stars stems from the nonorthogonality between the two level states of stars. Moreover, the distances between stars are also proven to play a key role in the entanglement for a symmetric multiqubit pure state. The number of unequal stars and the normalized product of the distance between stars perfectly match the classification and measure of the entanglement for a two- and three-qubit pure state, respectively, and thus can be taken as a tool of multiqubit entanglement. These results are closely connected to the symmetry of a quantum state. Therefore, the Majorana's stellar representation also has potential to be used to study other intriguing quantum issues, such as quantum transition and quantum tunneling.

ACKNOWLEDGMENTS

This work is supported by the National Fundamental Research Program of China (Contract No. 2013CBA01502), the National Natural Science Foundation of China (Contracts No. 11374040, No. 11575027, and No. 11405008), the Fundamental Research Funds for the Central Universities (Grant No. 2412015KJ009), and the Plan for Scientific and Technological Development of Jilin Province (Grant No. 20160520173JH).

[1] E. Majorana, Nuovo Cimento **9**, 43 (1932).
[2] J. Schwinger, in *Quantum Theory of Angular Momentum*, edited by L. Biendenham and H. Van Danm (Academic, New York, 1965).
[3] D. M. Stamper-Kurn and M. Ueda, Rev. Mod. Phys. **85**, 1191 (2013).
[4] B. Lian, T.-l. Ho, and H. Zhai, Phys. Rev. A **85**, 051606(R) (2012).
[5] X. Cui, B. Lian, T.-L. Ho, B. L. Lev, and H. Zhai, Phys. Rev. A **88**, 011601(R) (2013).
[6] R. Barnett, D. Podolsky, and G. Refael, Phys. Rev. B **80**, 024420 (2009).
[7] A. Lamacraft, Phys. Rev. B **81**, 184526 (2010).
[8] Y. Kawaguchi and M. Ueda, Phys. Rep. **520**, 253 (2012).
[9] A. R. Usha Devi, Sudha, and A. K. Rajagopal, Quantum Inf. Proc. **11**, 685 (2012).
[10] P. Ribeiro, J. Vidal, and R. Mosseri, Phys. Rev. Lett. **99**, 050402 (2007).
[11] P. Ribeiro, J. Vidal, and R. Mosseri, Phys. Rev. E **78**, 021106 (2008).
[12] M. V. Berry, Proc. R. Soc. London. Ser. A **392**, 45 (1984).
[13] B. Simon, Phys. Rev. Lett. **51**, 2167 (1983).
[14] D. Chruściński and A. Jamiołkowski, *Geometric Phases in Classical and Quantum Mechanics (Progress in Mathematical Physics)* (Birkhäuser, Boston, 2004), Vol. 36.
[15] A. Bohm, A. Mostafazadeh, H. Koizumi, Q. Niu, and J. Zwanziger, *The Geometric Phase in Quantum Systems* (Springer-Verlag, Berlin, 2003).
[16] J. H. Hannay, J. Phys. A **31**, L53 (1998).
[17] P. Bruno, Phys. Rev. Lett. **108**, 240402 (2012).
[18] S. Tamate, K. Ogawa, and M. Kitano, Phys. Rev. A **84**, 052114 (2011).
[19] H. D. Liu and L. B. Fu, Phys. Rev. Lett. **113**, 240403 (2014).
[20] K. Ogawa, S. Tamate, H. Kobayashi, T. Nakanishi, and M. Kitano, Phys. Rev. A **91**, 062118 (2015).
[21] V. Coffman, J. Kundu, and W. K. Wootters, Phys. Rev. A **61**, 052306 (2000).
[22] A. Miyake, Phys. Rev. A **67**, 012108 (2003).
[23] W. Dür, G. Vidal, and J. I. Cirac, Phys. Rev. A **62**, 062314 (2000).
[24] A. Acín, D. Bruß, M. Lewenstein, and A. Sanpera, Phys. Rev. Lett. **87**, 040401 (2001).
[25] A. Mandilara, T. Coudreau, A. Keller, and P. Milman, Phys. Rev. A **90**, 050302 (2014).
[26] M. Aulbach, D. Markham, and M. Murao, New J. Phys. **12**, 073025 (2010).
[27] D. J. H. Markham, Phys. Rev. A **83**, 042332 (2011).
[28] Z. Wang and D. Markham, Phys. Rev. Lett. **108**, 210407 (2012).
[29] Z. Wang and D. Markham, Phys. Rev. A **87**, 012104 (2013).
[30] W. Ganczarek, M. Kuś, and K. Życzkowski, Phys. Rev. A **85**, 032314 (2012).
[31] T. Bastin, S. Krins, P. Mathonet, M. Godefroid, L. Lamata, and E. Solano, Phys. Rev. Lett. **103**, 070503 (2009).
[32] P. Mathonet, S. Krins, M. Godefroid, L. Lamata, E. Solano, and T. Bastin, Phys. Rev. A **81**, 052315 (2010).
[33] P. Ribeiro and R. Mosseri, Phys. Rev. Lett. **106**, 180502 (2011).
[34] F. Bloch and I. I. Rabi, Rev. Mod. Phys. **17**, 237 (1945).
[35] C. T. Lee, J. Phys. A **21**, 3749 (1988).
[36] C. Yang, H. Guo, L.-B. Fu, and S. Chen, Phys. Rev. B **91**, 125132 (2015).
[37] M. Berry, in *Anomalies, Phases, Defects...*, edited by M. Bregola, G. Marmo, and G. Morandi (Bibliopolis, Naples, 1990), pp. 403–428.
[38] M. Hayashi, D. Markham, M. Murao, M. Owari, and S. Virmani, J. Math. Phys. **50**, 122104 (2009).
[39] W. K. Wootters, Phys. Rev. Lett. **80**, 2245 (1998).
[40] J. C. Loredo, M. A. Broome, D. H. Smith, and A. G. White, Phys. Rev. Lett. **112**, 143603 (2014).
[41] D. Greenberger, M. Horne, and A. Zeilinger, *Bell's Theorem, Quantum Theory, and Conceptions of the Universe*, edited by M. Kafatos (Kluwer, Dordrecht, 1989).
[42] M. Aulbach, arXiv:1103.0271.

[43] J. I. Cirac, M. Lewenstein, K. Mølmer, and P. Zoller, Phys. Rev. A **57**, 1208 (1998).
[44] A. Leggett, Rev. Mod. Phys. **73**, 307 (2001).
[45] J. Ma, X. Wang, C. Sun, and F. Nori, Phys. Rep. **509**, 89 (2011).
[46] S. Raghavan, A. Smerzi, and V. M. Kenkre, Phys. Rev. A **60**, R1787 (1999).
[47] A. P. Tonel, J. Links, and A. Foerster, J. Phys. A **38**, 1235 (2005).
[48] G. J. Milburn, J. Corney, E. M. Wright, and D. F. Walls, Phys. Rev. A **55**, 4318 (1997).
[49] A. Smerzi, S. Fantoni, S. Giovanazzi, and S. R. Shenoy, Phys. Rev. Lett. **79**, 4950 (1997).